Performance of Software-Based Solar Adaptive Optics System

Noriaki Miura [*], Yuuki Noto, Shuusuke Kato, Susumu Kuwamura, Naoshi Baba [1], Yoichirou Hanaoka [2], Satoru Ueno [3], and Reizaburou Kitai [3]

Department of Computer Sciences, Kitami Institute of Technology, 165 Koen-cho, Kitami, Hokkaido 090-8507, Japan

[1] Department of Applied Physics, Graduate School of Engineering, Hokkaido University, Sapporo, 060-8628, Japan

[2] National Astronomical Observatory, 2-21-1 Osawa, Mitaka, Tokyo 181-8588, Japan

[3] Hida Observatory, Graduate School of Science, Kyoto University, Kamitakara, Takayama, Gifu 506-1314, Japan

Abstract

This short note reports the performance of our modified adaptive optics system for solar observations. This system operates at a frame rate of about 400 Hz and has the closed-loop cutoff frequency at 105 Hz. The results of the laboratory experiments show that this system compensates for a temporal wavefront-variation of less than 99 Hz and improves the Strehl ratio by a factor of five.

KEYWORDS: adaptive optics, solar observation

[*] E-mail address: miura@cs.kitami-it.ac.jp

We earlier reported our solar adaptive optics (AO) system [1)], where commercially available devices and standard personal computers are used. In contrast to other AO systems [2-8)], our system is designed to compensate for low-order turbulence in rather short wavelength for the domeless solar telescope at the Hida Observatory in Japan. We modified our AO system for solar observations in 2006. In this note, we show the temporal property and the imaging performance of this modified AO system. The theoretical temporal property and the experimental imaging performance were not treated in the previous paper [1)].

Two modifications have been made to improve our AO system. The optical setup was redesigned to exclude insignificant optical components used in the previous system. Figure 1 shows our modified AO system. This redesign of the optical setup has advantages of both suppressing aberration and avoiding light loss. By virtue of the latter, we could set the exposure time to 0.41 ms, which is shorter than that in the previous system. The other modification is optimization of the software. We rewrote and removed inefficient software codes, and replaced floating point executions with integer ones. The working frequency thus rose to 400 Hz for both wavefront and tip-tilt compensations, whereas it was 250 Hz in the previous system.

Our AO system is a standard closed-loop type and hence its output transfer function can be theoretically derived as written in the ref. 9. We numerically calculated the transfer function to obtain the Bode diagram. From the Bode diagram in Fig. 2, we estimated the -3 dB closed-loop cutoff-frequency at 105 Hz.

We set up a simulated atmosphere-telescope system in our laboratory, where a

deformable mirror, referred to as a turbulence mirror, causes turbulence on the wavefront from a He-Ne laser, a pinhole acts as an object, and a lens functions as a primary mirror of the telescope. We can tune the frequency of turbulence by changing a software parameter. We conducted experiments by putting our AO module behind the simulated atmosphere-telescope system.

The first experiment was conducted to check the performance of tip-tilt compensation: the surface of the turbulence mirror was kept flat but its tilt was changed at a given oscillation frequency. We calculated the deviations of temporal variation in centroid positions of the laser spot. Table 1 summarizes the results of experiments with various oscillation frequencies. One can confirm the effect of tip-tilt compensation up to 96 Hz. However, the use of AO was not effective in compensating turbulence of higher frequencies than 208 Hz.

In the second experiment, we investigated the temporal behavior of turbulence compensation. The surface of the turbulence mirror was deformed at a given frequency. We measured the normalized correlation values of every two neighboring images of the laser spot, and then calculated their average. If the AO system worked perfectly, cross-correlation values between frames should always be unity. Columns 2 and 3 in Table 2 list the average cross-correlation values of images obtained without and with AO, respectively. Up to 99 Hz, their values reasonably increased by the use of AO, while they became worse beyond 217 Hz. A good agreement was observed between the values experimentally determined (99 Hz) and those theoretically derived (105 Hz).

To examine the imaging performance of our AO system, we also added 200 turbulent images to make a long-exposure image, and then calculated its Strehl ratio. We defined this as the ratio of the maximum to the total intensity of a PSF. Figure 3(a)

shows a spot image without any turbulence, while (b) is the long-exposure image obtained under turbulence of 32 Hz. Figures 3(c) and (d) show the long-exposure images when the AO system was applied to the turbulence of 32 and 172 Hz, respectively. The Strehl ratios are summarized in columns 4 and 5 in Table 2, where the values are normalized so as to make the value of (a) unity. As predicted, the Strehl ratios became worse as the turbulence frequency was made to rise. However, when the turbulence frequency was less than the cutoff frequency of 105 Hz, the Strehl ratio was improved by a factor of more than five.

We made solar observations at the Hida Observatory in September, 2006. The observational wavelength and bandwidth were 650 nm and 50 nm, respectively. Figure 4(a) is the long-exposure sunspot image viewed without AO at 10:25, September 8, 2006, in JST. The field of view of this image is 30.7x30.7 arcsec^2, and fine structures, such as solar granulation, can hardly been recognized because of atmospheric turbulence. We measured the seeing condition with our wavefront sensor and obtained the value of D/r0=14.12 at 10:28. On the other hand, using AO improved the image quality as shown in Fig. 4(b). The observational time of this image was 10:27. The image contrast except for the region around the sunspot rose from 0.036 to 0.041 by the use of AO, where the contrast is defined as the ratio of variance of pixel values to their average.

This work was partially supported by both a Grant-in-Aid for Scientific Research (C) from the Japan Society for the Promotion of Science (No.17540209) and a foundation for university support from the National Astronomical Observatory of Japan.

References

1. N. Miura, T. Kobayashi, S. Sakuma, S. Kuwamura, N. Baba, Y. Hanaoka, S. Ueno, and R. Kitai: Opt. Rev. **13** (2006) 338.
2. R. B. Dunn: Proc. SPIE **1271** (1990) 216.
3. D. S. Acton and R. C. Smithson: Appl. Opt. **31** (1992) 3161.
4. G. B. Scharmer, P. Dettori, M. G. Löfdahl, and M. Shand: Proc. SPIE **4853** (2003) 370
5. T. R. Rimmele and R. R. Radick: Proc. SPIE **3353** (1998) 72.
6. T. Berkefeld, D. Soltau, and O. von der Lühe: Proc. SPIE **5903** (2005) 59030O.
7. C. Paterson, I. Munro, and J. C. Dainty: Opt. Express **6** (2000) 175.
8. C. U. Keller, C. Plymate, and S. M. Ammons: Proc. SPIE **4853** (2003) 351.
9. P.-Y. Modec: in *Adaptive Optics in Astronomy* ed. F. Roddier (Cambridge University Press, Cambridge, 1999) *Chap. 6*.

Table 1. Deviations of centroid positions

Oscillation frequency (Hz)	Without AO		With AO	
	Horizontal (pixels)	Vertical (pixels)	Horizontal (pixels)	Vertical (pixels)
32	3.49	0.23	0.73	0.36
64	3.51	0.26	1.37	0.40
96	3.52	0.24	2.89	0.73
127	3.51	0.23	2.79	0.71
167	3.62	0.23	3.51	0.91
208	3.47	0.26	5.76	1.94
252	3.67	0.27	7.60	1.59

Table 2. Results of wavefront compensation

Turbulence frequency (Hz)	Average cross-correlation values		Strehl ratios	
	Without AO	With AO	Without AO	With AO
32	0.63	0.92	0.12	0.75
66	0.66	0.90	0.12	0.67
99	0.67	0.83	0.12	0.58
130	0.67	0.72	0.11	0.40
172	0.67	0.73	0.11	0.27
217	0.65	0.65	0.11	0.19
262	0.69	0.59	0.11	0.13

Figure Captions

Figure 1. Optical setup of the modified solar adaptive optics system.

Figure 2. Bode diagram specifying the temporal property of the AO system.

Figure 3. Long-exposure images of the laser spot: (a) without any turbulence, (b) with turbulence of 32 Hz, (c) and (d) with application of AO to turbulence of 32 Hz and 172 Hz, respectively.

Figure 4. Long-exposure solar images observed (a) without and (b) with AO.

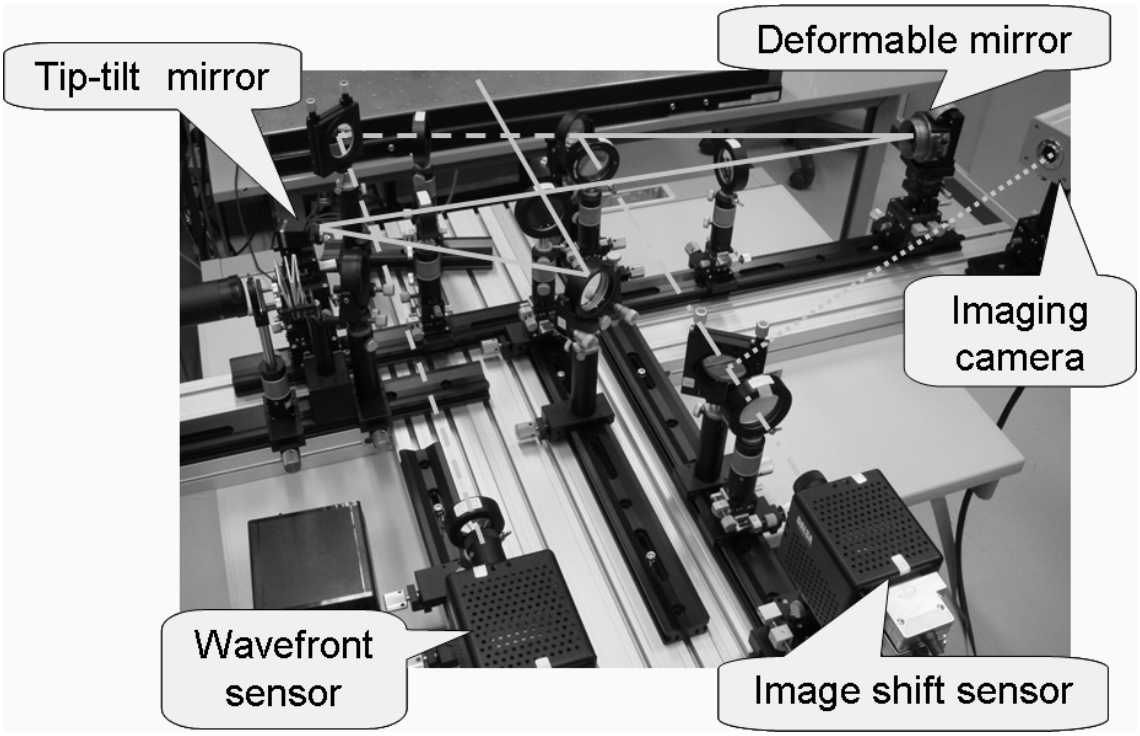

Figure 1. N. Miura

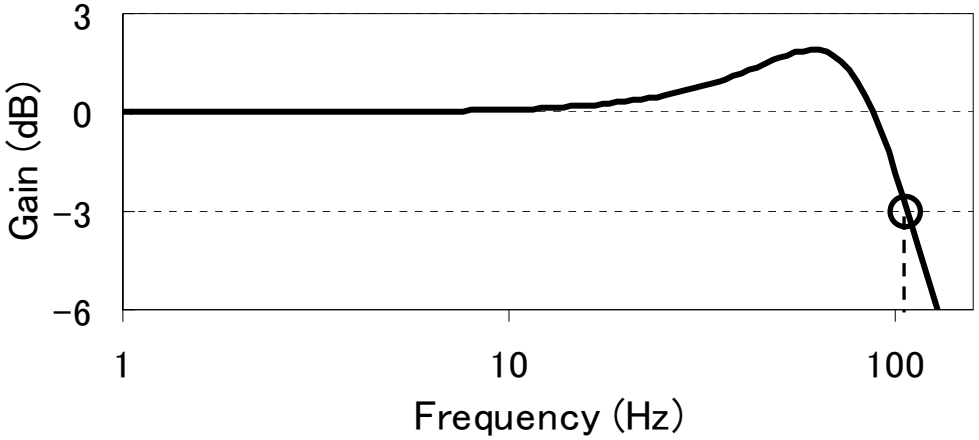

Figure 2. N. Miura

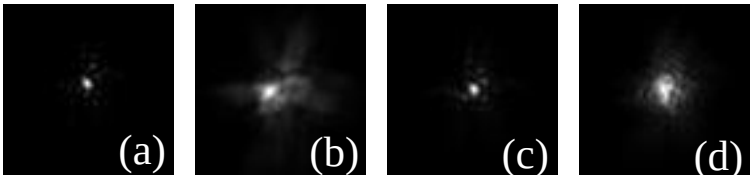

Figure 3. N. Miura

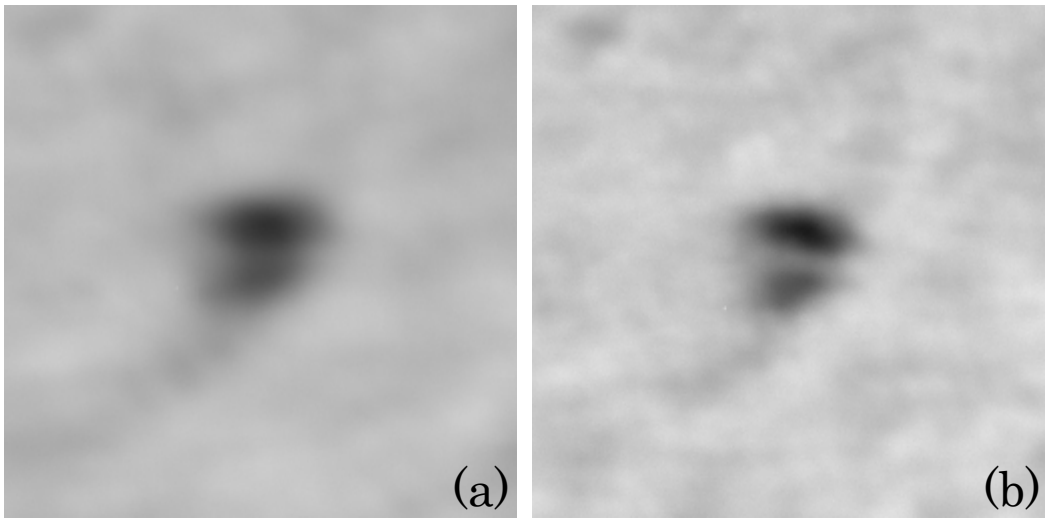

Figure 4. N. Miura